

Probing Materials' Behavior using Fast Electrons

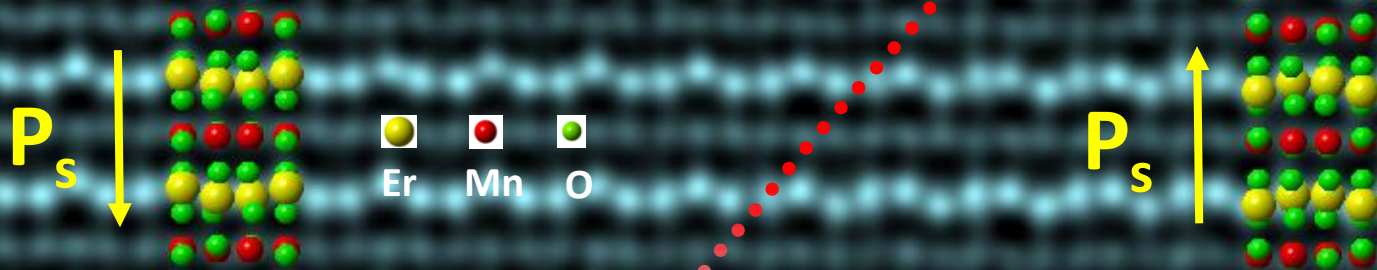
Yimei Zhu

Dept. of Condensed Matter Physics
Brookhaven National Laboratory
Long Island, NY 11973

Workshop on Ultrafast
Dec 9-12, 2013, Key West, FL



180° ferroelectric domain wall in multiferroic ErMnO_3

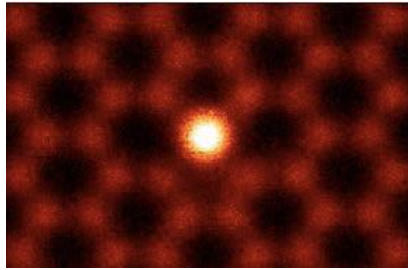


1 nm

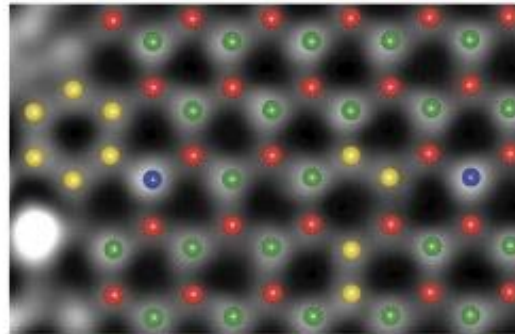
MG. Han /BNL

Imaging atoms

Single Si atom on graphene

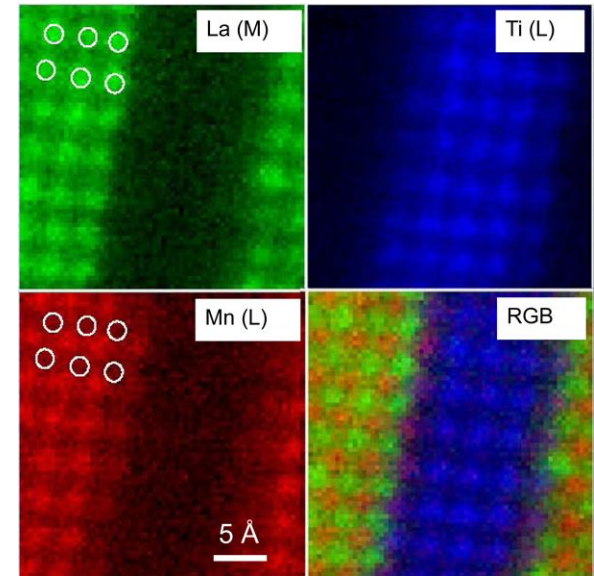


Single BN layer



red: B; yellow: C; green: N; blue: O

EELS mapping: $\text{La}_{0.7}\text{Sr}_{0.3}\text{MnO}_3/\text{SrTiO}_3$



Muller et al Science 319, 1073 (2008)

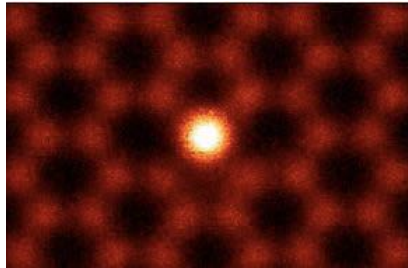


Krivanek et al, Nature (2010)

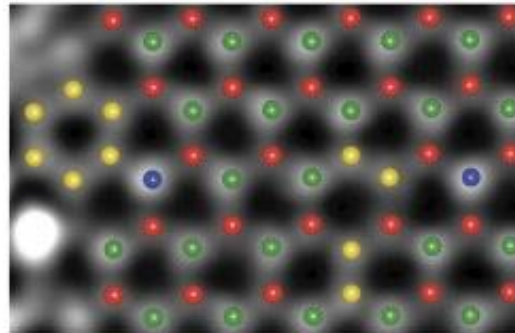


Imaging atoms

Single Si atom on graphene



Single BN layer

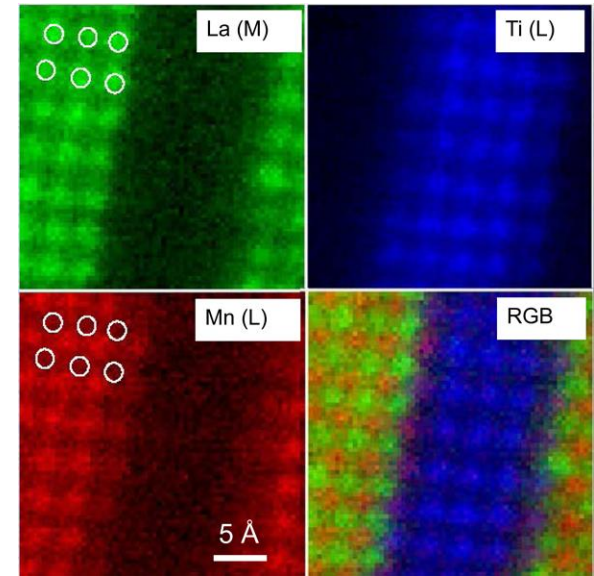


red: B; yellow: C; green: N; blue: O



Krivanek et al, Nature (2010)

EELS mapping: $\text{La}_{0.7}\text{Sr}_{0.3}\text{MnO}_3/\text{SrTiO}_3$



Muller et al Science 319, 1073 (2008)

PRL 111, 046101 (2013)

Selected for a **Viewpoint** in *Physics*
PHYSICAL REVIEW LETTERS

week ending
26 JULY 2013

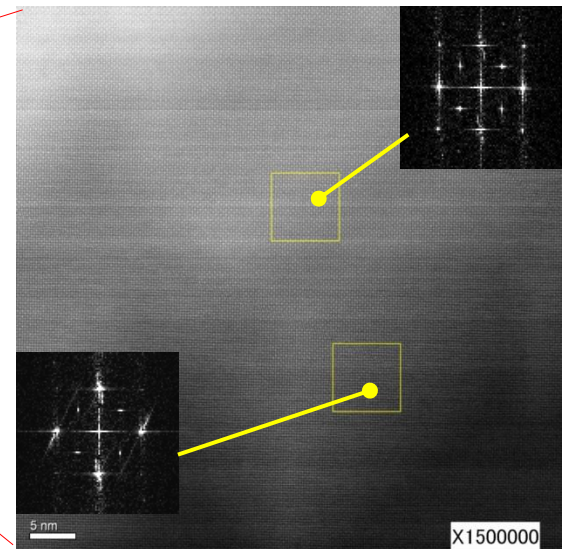
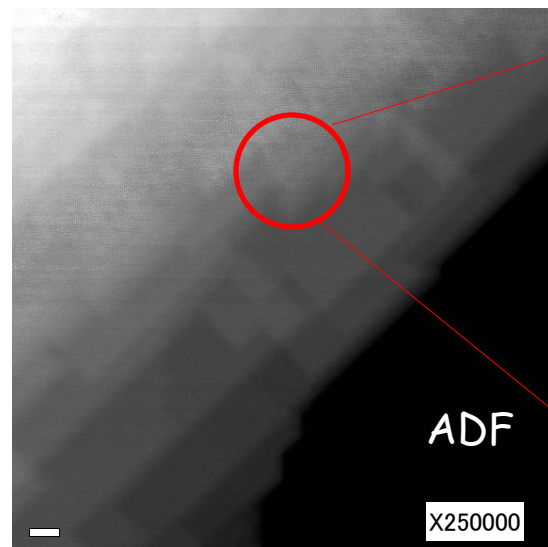
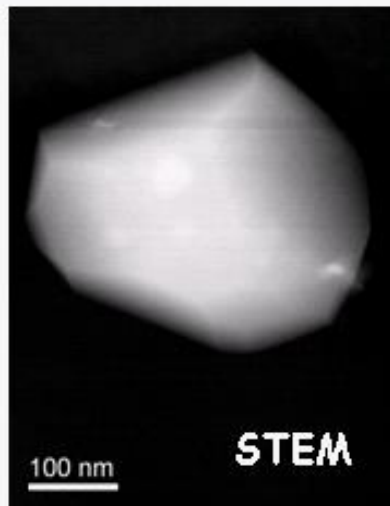
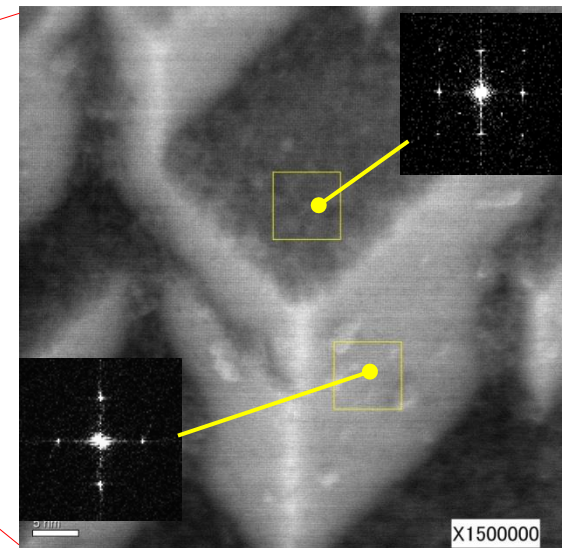
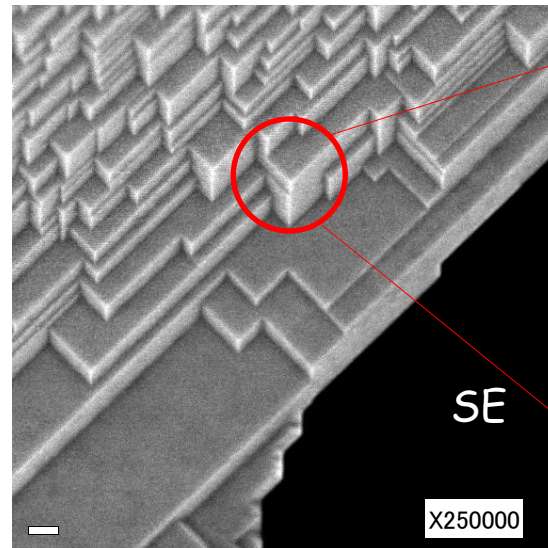
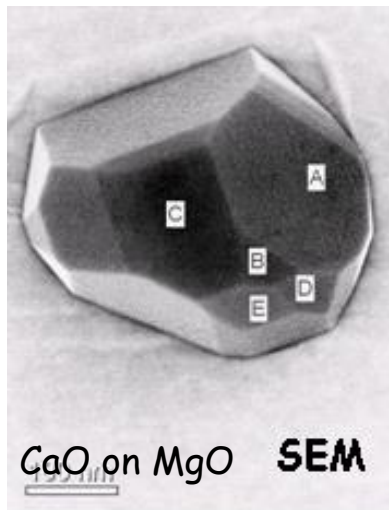


Thermal Magnetic Field Noise Limits Resolution in Transmission Electron Microscopy

Stephan Uhlemann,* Heiko Müller, Peter Hartel, Joachim Zach, and Max. Haider
CEOS Corrected Electron Optical Systems GmbH, Englerstraße 28, 69126 Heidelberg, Germany
(Received 6 May 2013; published 22 July 2013)

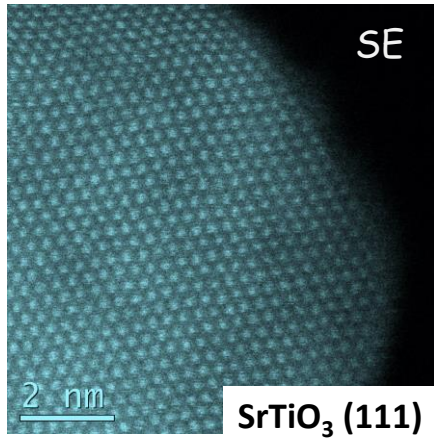
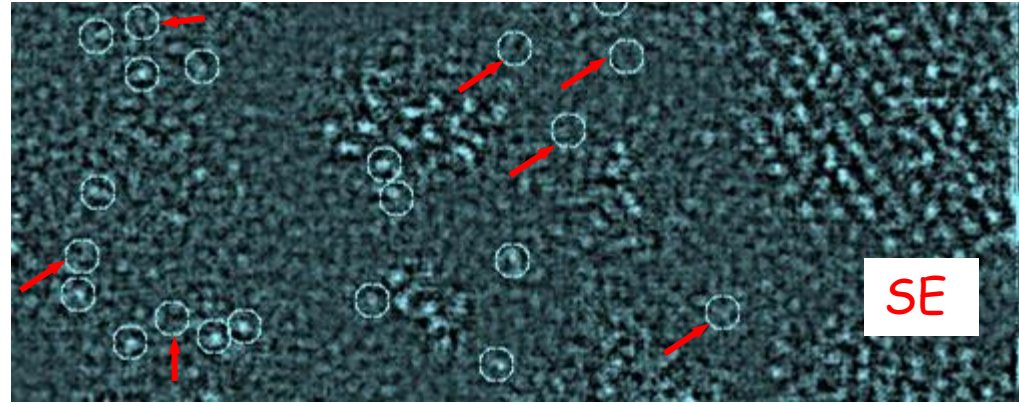
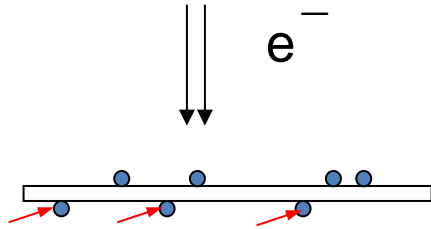
Atomic surface imaging with secondary electrons

SrTiO_3



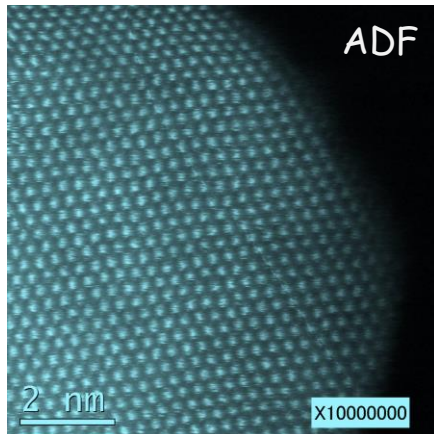
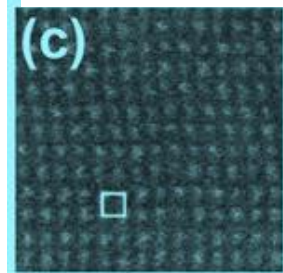
Atomic surface imaging with secondary electrons

Zhu, et al, Nature Materials, 8, 808 (2009)

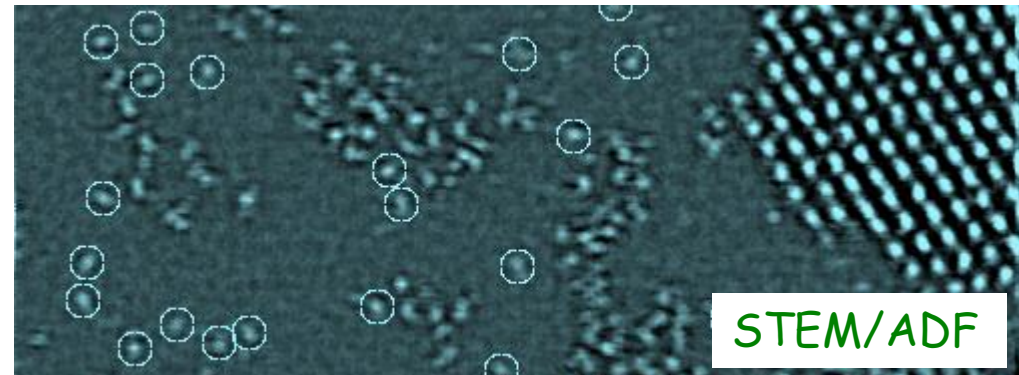


SrTiO_3 (001)

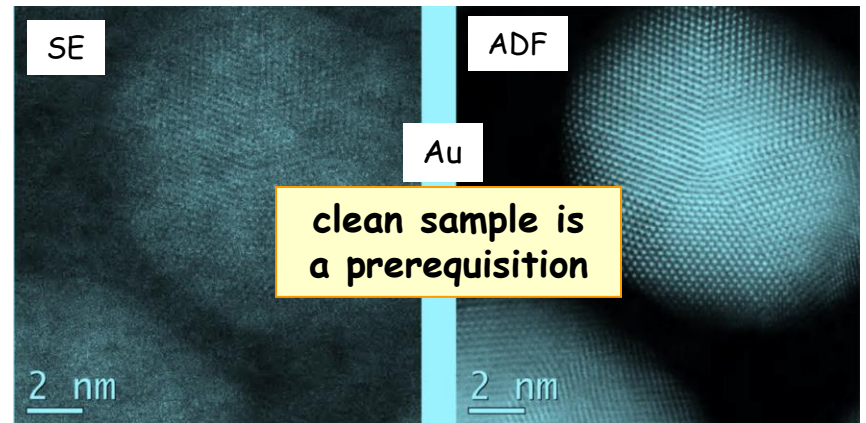
SrO terminated



TiO₂ terminated



Imaging surface U atoms



Uniqueness of electron scattering

Sensitive to valence electrons at small scattering angles

Mott formula

$$f^e = \frac{2\pi m_0 e^2}{h^2 \epsilon_0} \left(\frac{\lambda}{\sin \theta} \right)^2 (Z - f_x)$$

Electrons interact with electrostatic potential

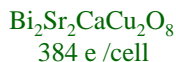


valence electrons

X-rays interact with electron cloud



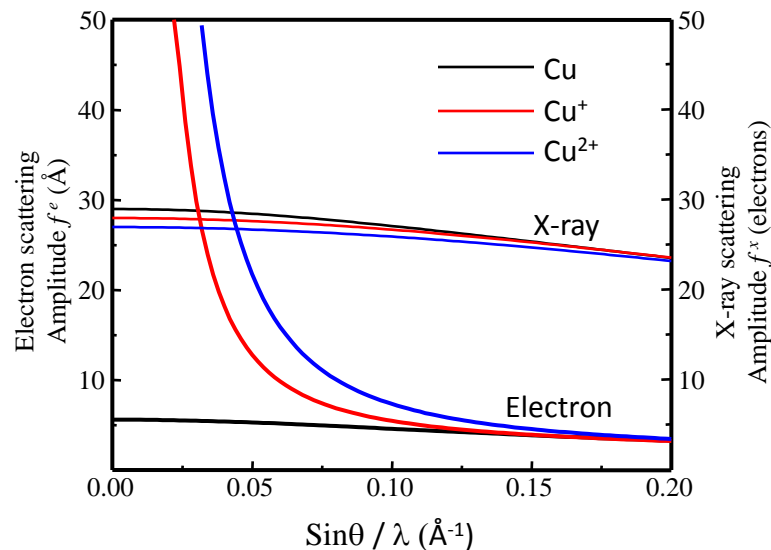
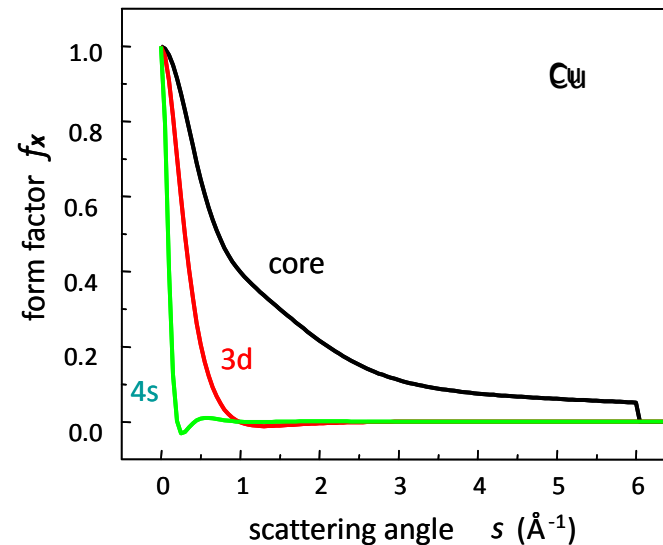
total electrons



difficulties for x-ray suitability criterion

$$\alpha = \frac{V}{\sum n^2} \gg 0.1 \sim 5$$

P. Coppens, (1997), "X-ray charge densities & chemical bonding"



Direct Imaging of Charge Modulation

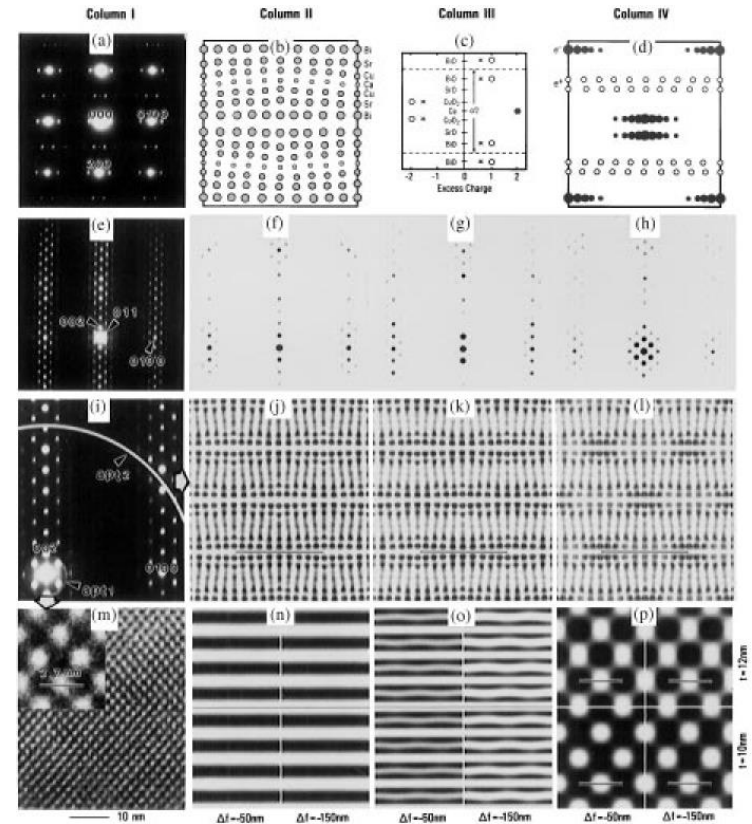
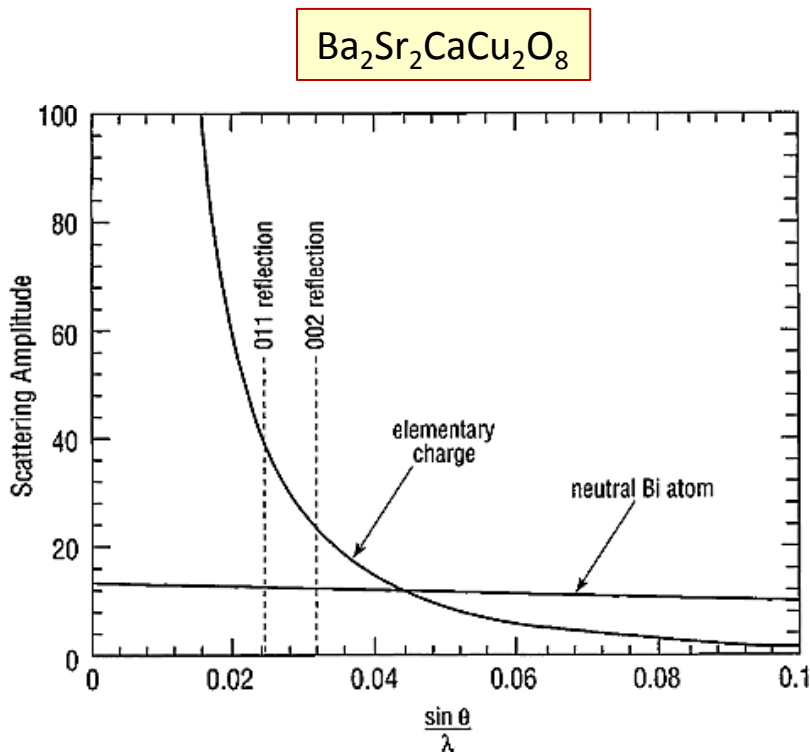
Yimei Zhu

Department of Applied Science, Brookhaven National Laboratory, Upton, New York 11973

J. Taftø

Department of Physics, University of Oslo, P.O. Box 1048, 0316 Blindern, Oslo 3, Norway

(Received 7 September 1995)



Picometer Accuracy in Measuring Lattice Displacements Across Planar Faults by Interferometry in Coherent Electron Diffraction

Lijun Wu, Yimei Zhu,* and J. Tafto†

Materials Science Division, Brookhaven National Laboratory, Upton, New York 11973

(Received 12 June 2000)

Physical Review Focus

Picometer Accuracy in Measuring Lattice Displacements Across Planar Faults by Interferometry in Coherent Electron Diffraction
Lijun Wu, Yimei Zhu, and J. Tafto
Phys. Rev. Lett. **85**, 5126 (11 December 2000)

The Most Accurate Defect Measurement

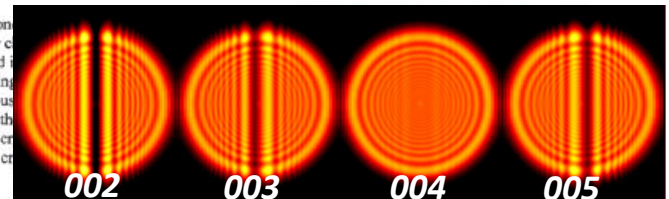
11 December 2000

Fault lines between pure crystals affect con-
properties of semiconductors in computer c
them precisely. A new technique, reported
electron beam to measure so-called stacking
meter (1 pm), ten times better than previous
purity of a coherent electron beam, the auth
transmitted through large regions of pure cr
technique may improve understanding of cr
with material properties.

Conventional electron microscopes use incoherent beam
heating a filament, so the electron waves originating fr
filament are not synchronized. But coherent beams con
from which the electrons are liberated by an electric fic
coherently from such a source, just as light streaming t
is more coherent than that of a lightbulb. Coherent elec
become commercially available in just the past five yer

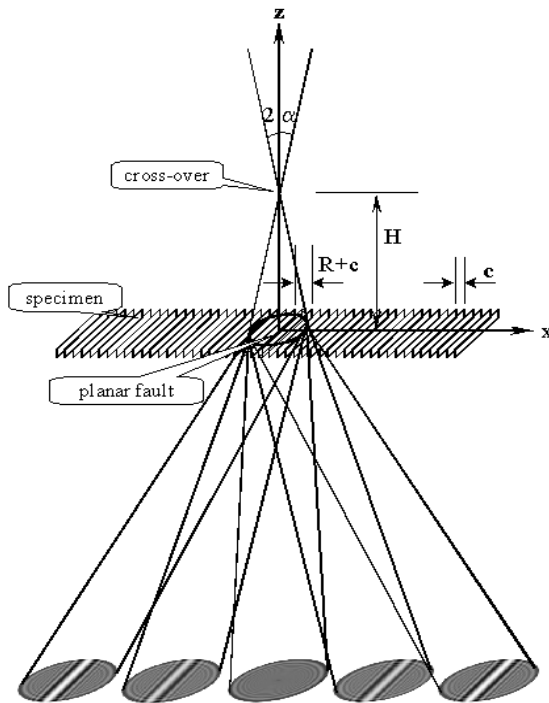
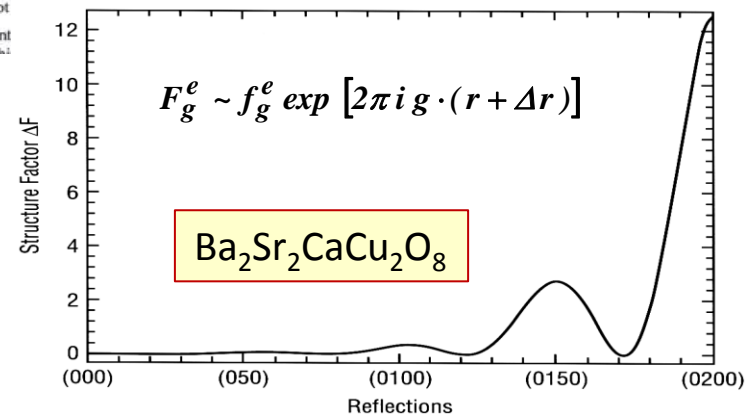
With improvements in coherent electron sources has ce
structures. The latest system, developed by Yimei Zhu
uses one of the best electron microscopes in the world,
the measurement does not

To make the measurement
obtainable high quality shi



$$g \cdot R = n$$

Accuracy : 0.01 Å



$$\varphi_g = \sum_{m,n} F_g \exp 2\pi i \left(\frac{\sqrt{r^2 + H^2}}{\lambda} - \vec{r} \cdot \vec{g} \right)$$

Imaging electrons, spins, electromagnetic potentials

Valence electron distribution

charge density ρ :

$$\rho(r) = \frac{1}{\Omega} \sum_g F_g^x \exp(2\pi i g \cdot r)$$

structure factor

$$\rho = -\nabla^2 V \epsilon_0$$

Electrostatic and magnetic potential distribution

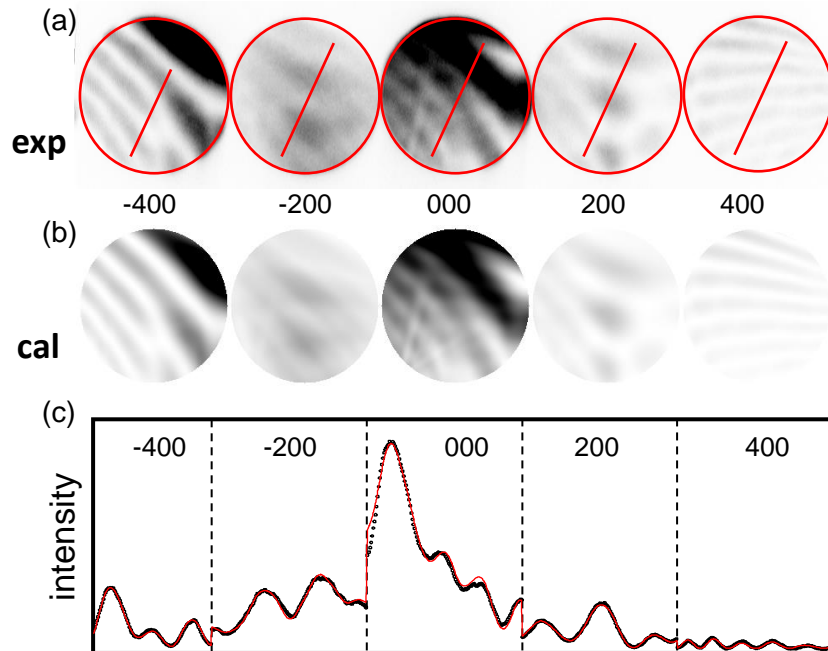
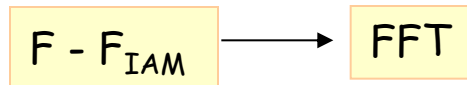
electrostatic potential V
magnetic potential B :

$$\phi(r) = C_E \int V(r, z) dz - \int \frac{e}{\hbar} \vec{A}(r, z) \cdot d\vec{r}$$

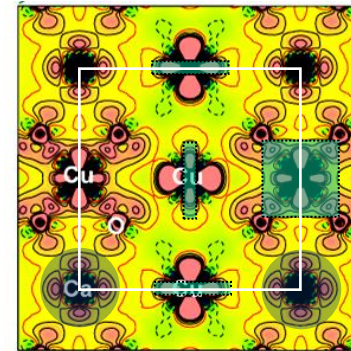
Aharonov-Bohm phase shift
of the wave function

Mapping valence electron distribution with quantitative diffraction

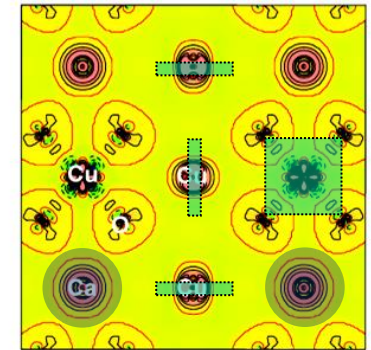
$$\rho(r) = \frac{1}{\Omega} \sum_g F_g^x \exp(2\pi i g \cdot r)$$



CaCu₃Ti₄O₁₂: PRL 99 037602 (2007)

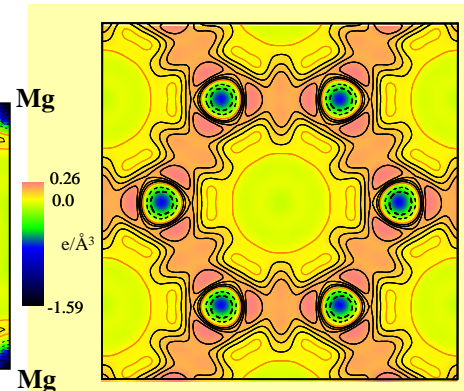
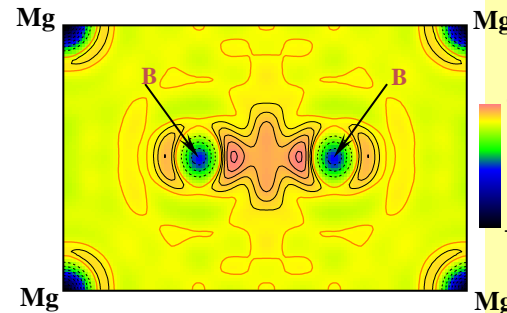


Experiment : ED + X-ray, 90K



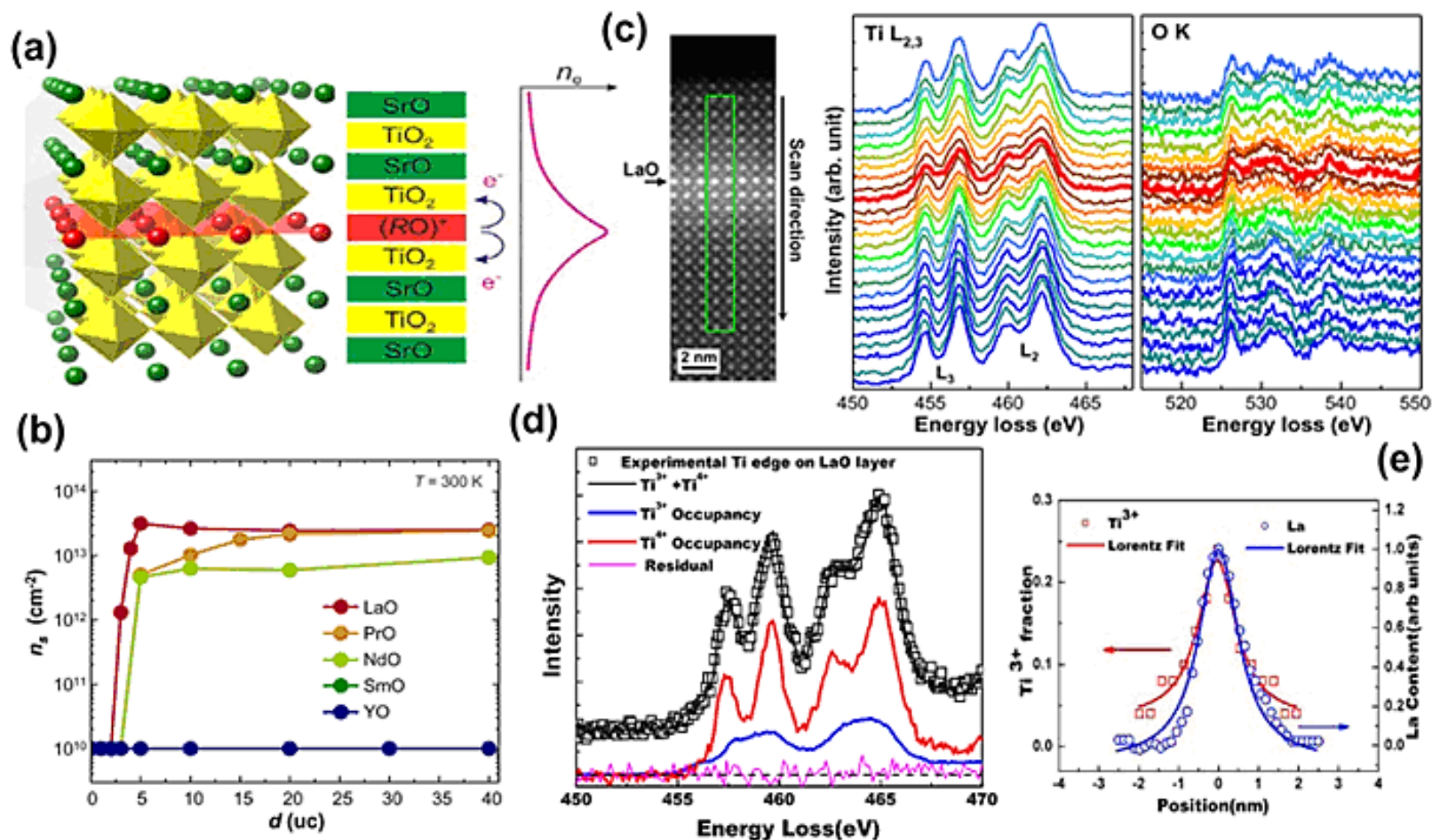
DFT, w/o disorder

MgB₂: PRL 88 247002 (2002)
PRB 69 064501 (2004)



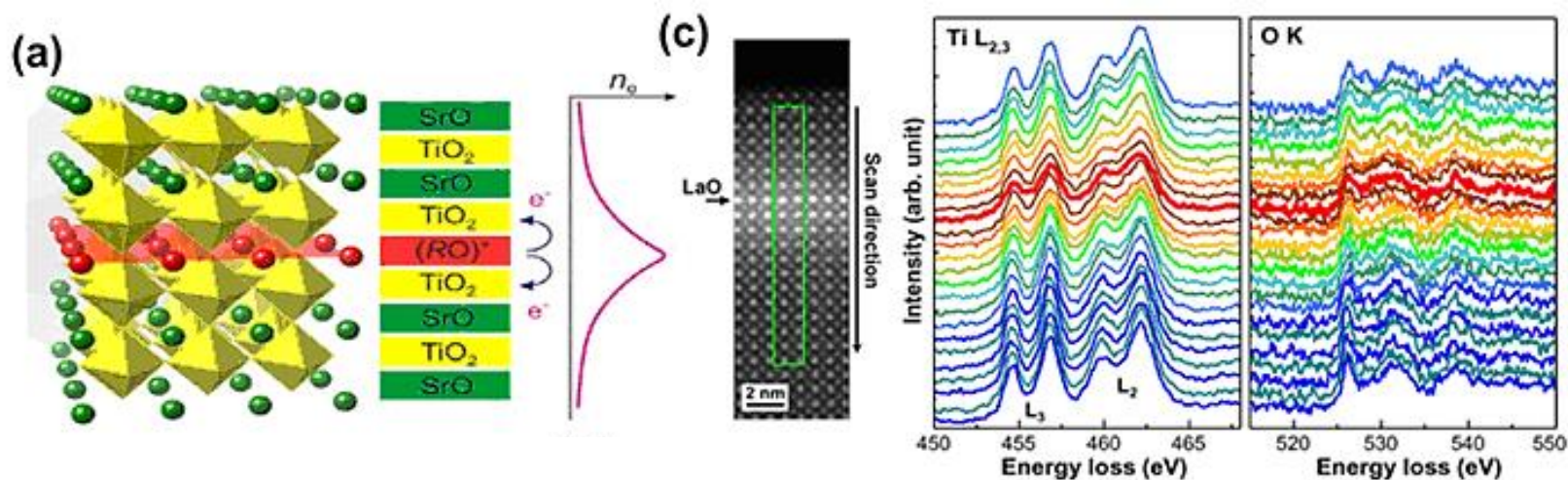
Probing bonding states and charge transfer with EELS

2-D Electron Gas: SrTiO₃/RO/SrTiO₃ (R=La, Pr, Nd, Sm, Y)

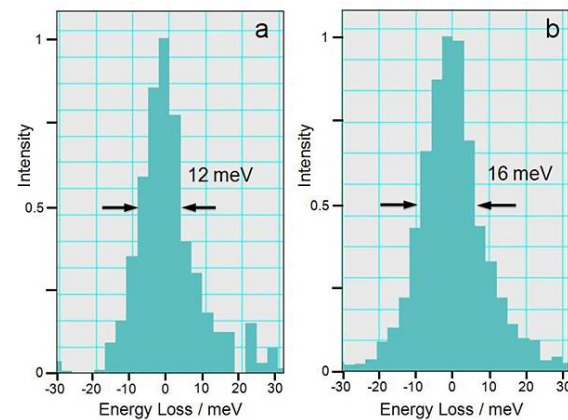
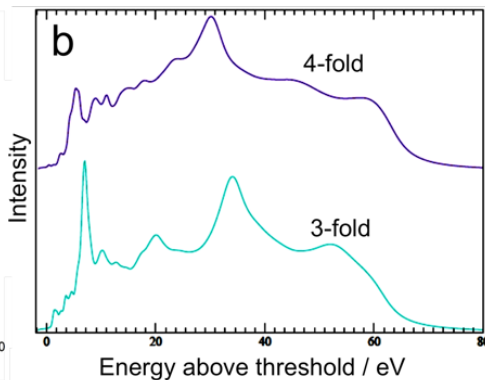
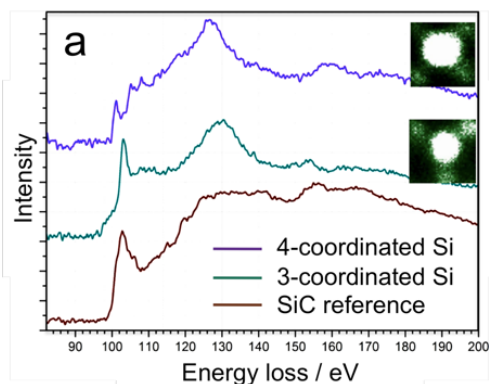


Probing bonding states and charge transfer with EELS

2-D Electron Gas: $\text{SrTiO}_3/\text{RO}/\text{SrTiO}_3$ (R=La, Pr, Nd, Sm, Y)



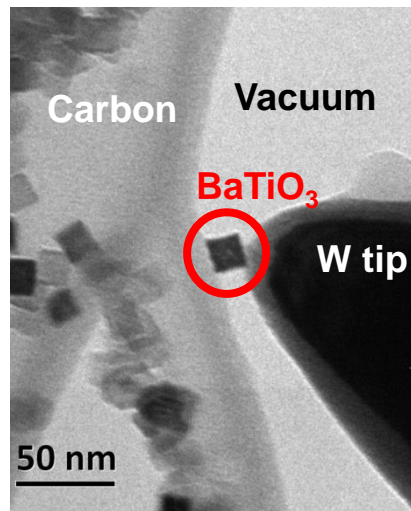
individual Si substitutional atoms on SiC



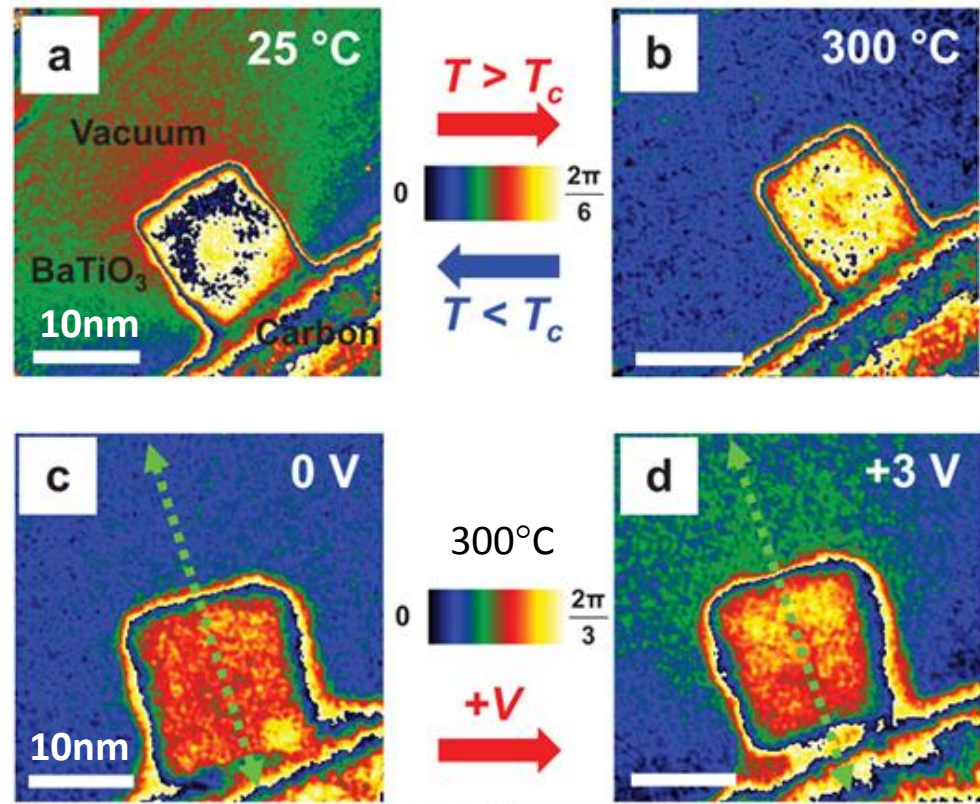
Direct imaging of ferroelectric order using holography

- RT ferroelectric order can be down to 10-15nm, below 10nm superparaelectric.

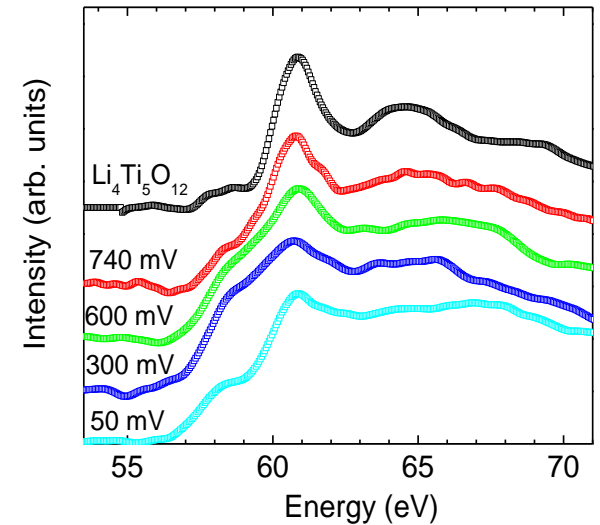
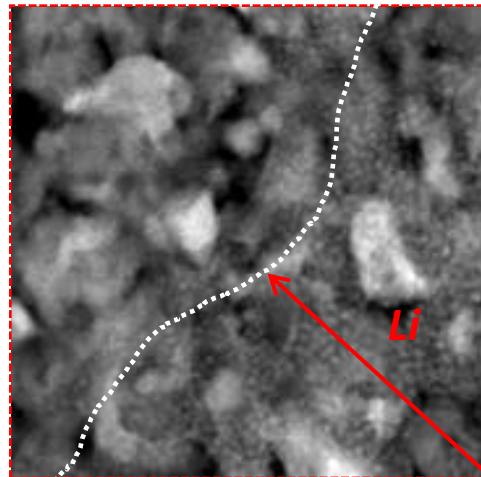
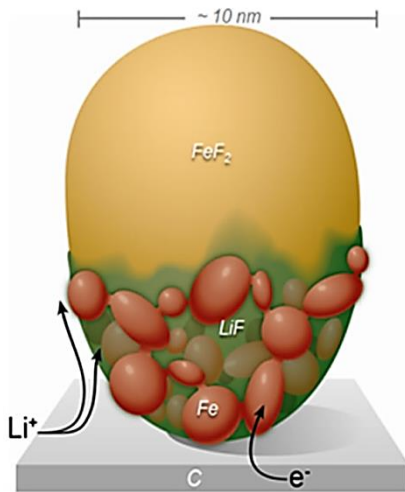
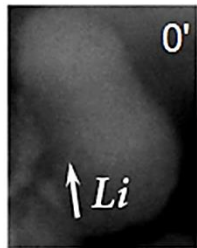
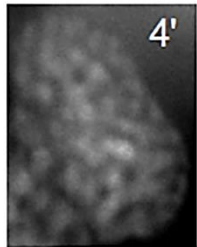
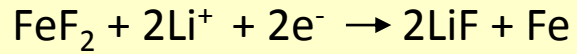
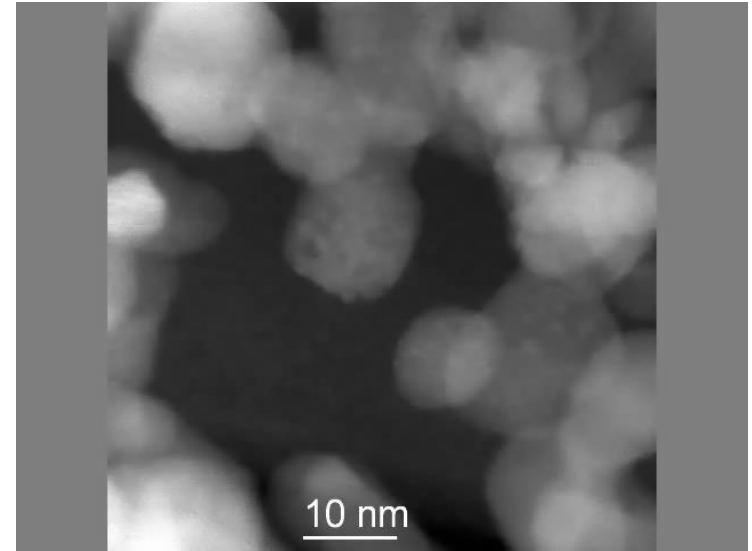
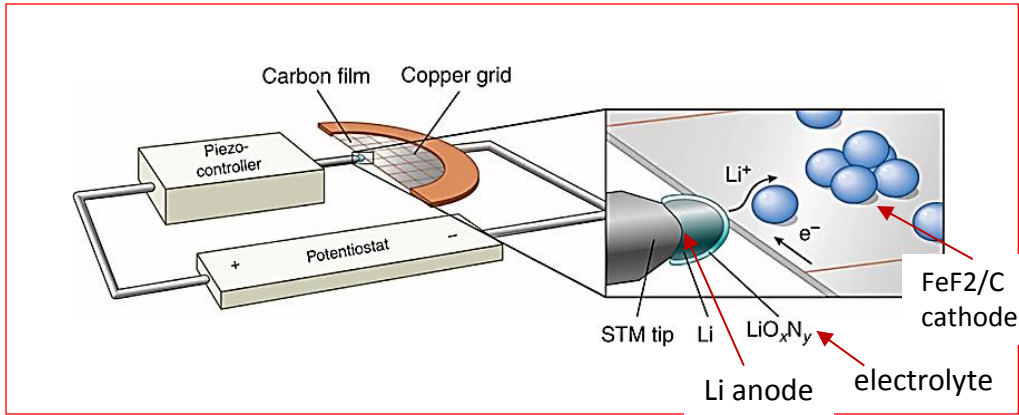
BaTiO₃
Curie temperature 130°C



Polking, Han, et al,
Nat. Mat., **11** 700 (2012)

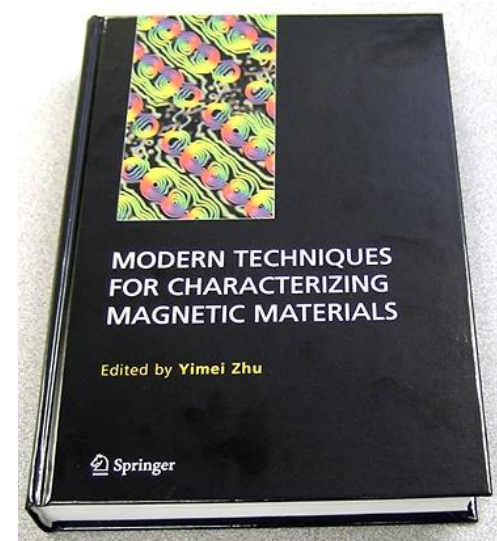


Direct observation of the Lithiation process in Li-ion-batteries



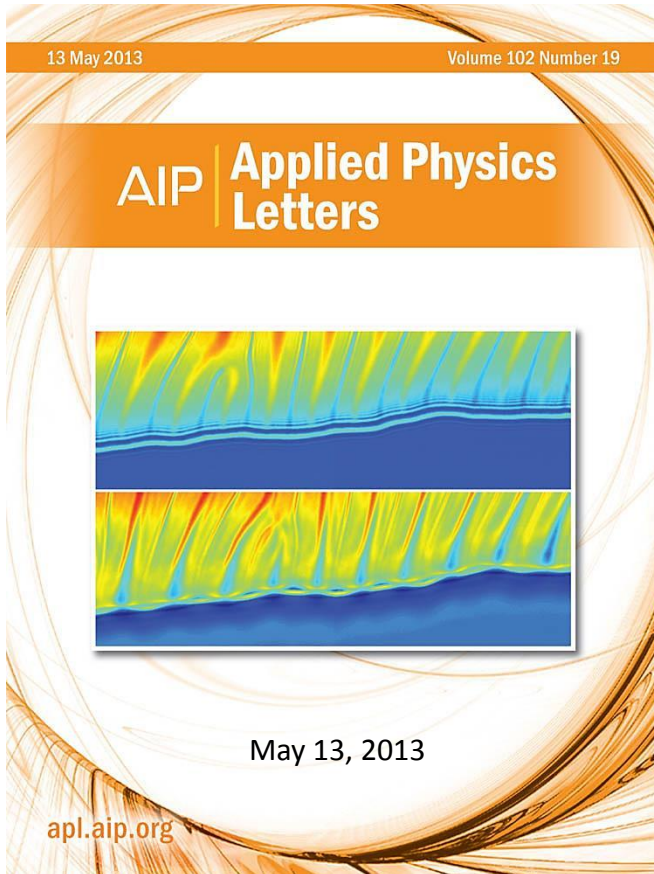
Can we image individual spins ?

For BCC Fe NP, the max phase shift is $\sim 50 \mu\text{rad}$, 10^{-3} of $2\pi/100$

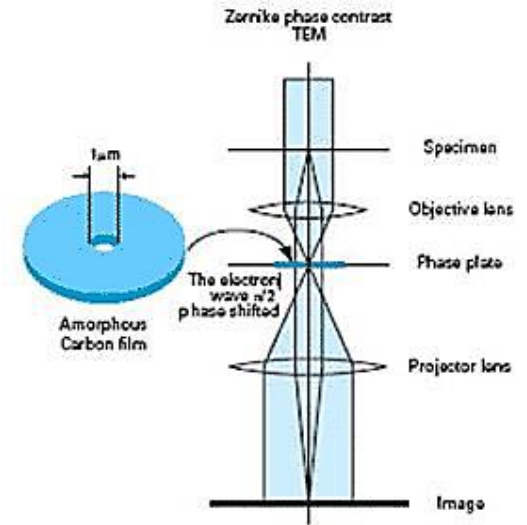
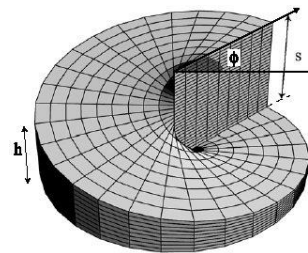
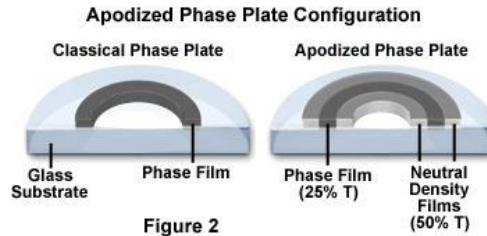


	EH	LM	MFM	SP-STM	n	MOKE	X-rays
Strength	Mapping fields, measuring moments	Quick and easy, large field of view	Easy, cheap	Single-spin sensitivity, manipulation	Resolving unknown spin structures, spin wave $Q(w)$	Super fast dynamics	Super fast dynamics
Weakness	Requires practice	Qualitative	Perturbs sample	Surface-only	Bulk/crystal-only, requires a neutron source	Surface-only	Requires a synchrotron
Time resolution	100 ms	10 ms	1 s	1 s	n/a	1 fs	1 fs
Spatial resolution	3 nm	10 nm	50 nm	0.1 nm	n/a	100 nm	20 nm
Sensitivity	$\pi/100$ rad phase shift	$1 \mu\text{rad}$ deflection	100 pN force	$<1 \mu_B$ moment	$<1 \mu_B$ moment	$20 \mu\text{rad}$ rotation	?

Phase plate for magnetic imaging



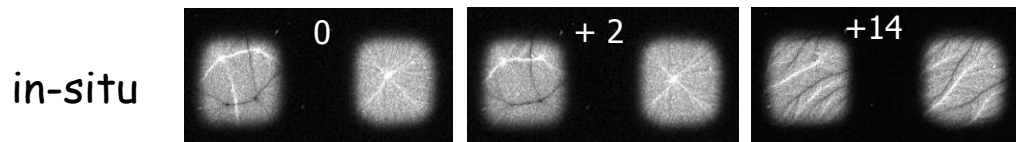
Zernike phase plate:
convert phase contrast to
amplitude contrast



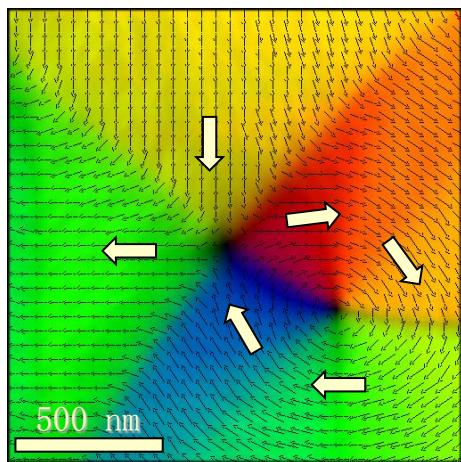
Pollard, Malac, Belleggia, Kawasaki, Zhu
APL 102, 192401 (2013)

Hole free Phase Plate

Imaging magnetic moments

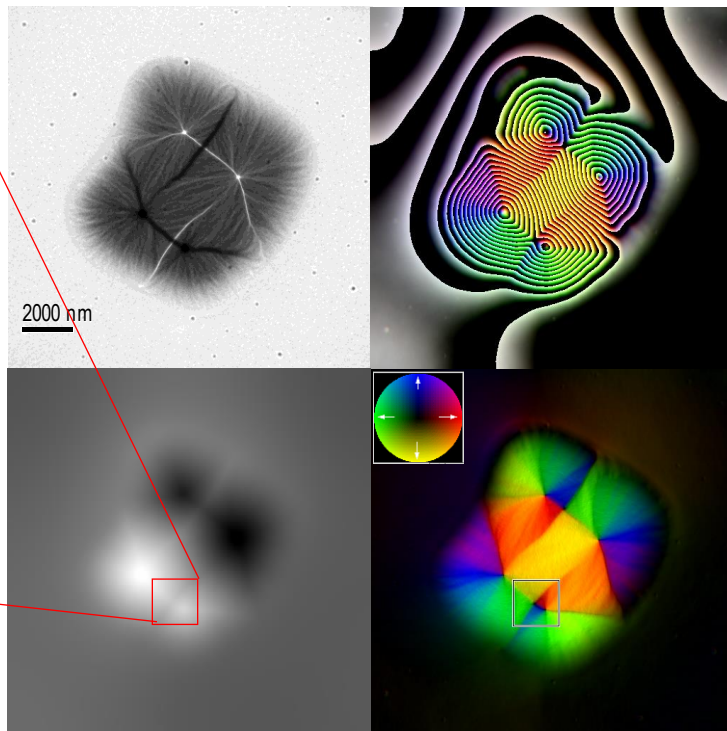


vortex & antivortex



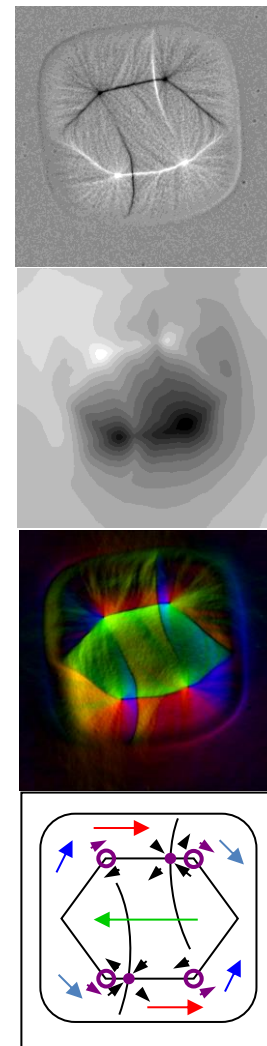
magnetization
vector map

Lorentz contrast



phase image

V.Volkov and Y. Zhu
PRL. 91 043904(2003)

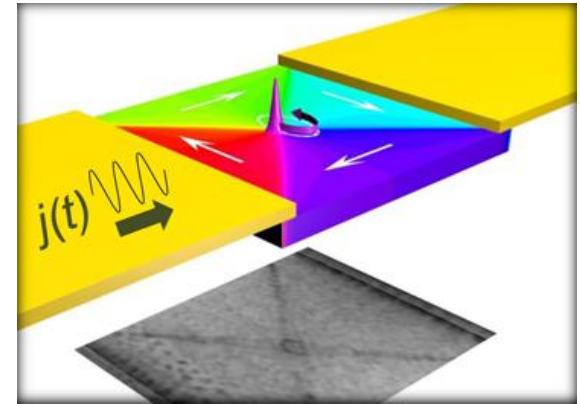
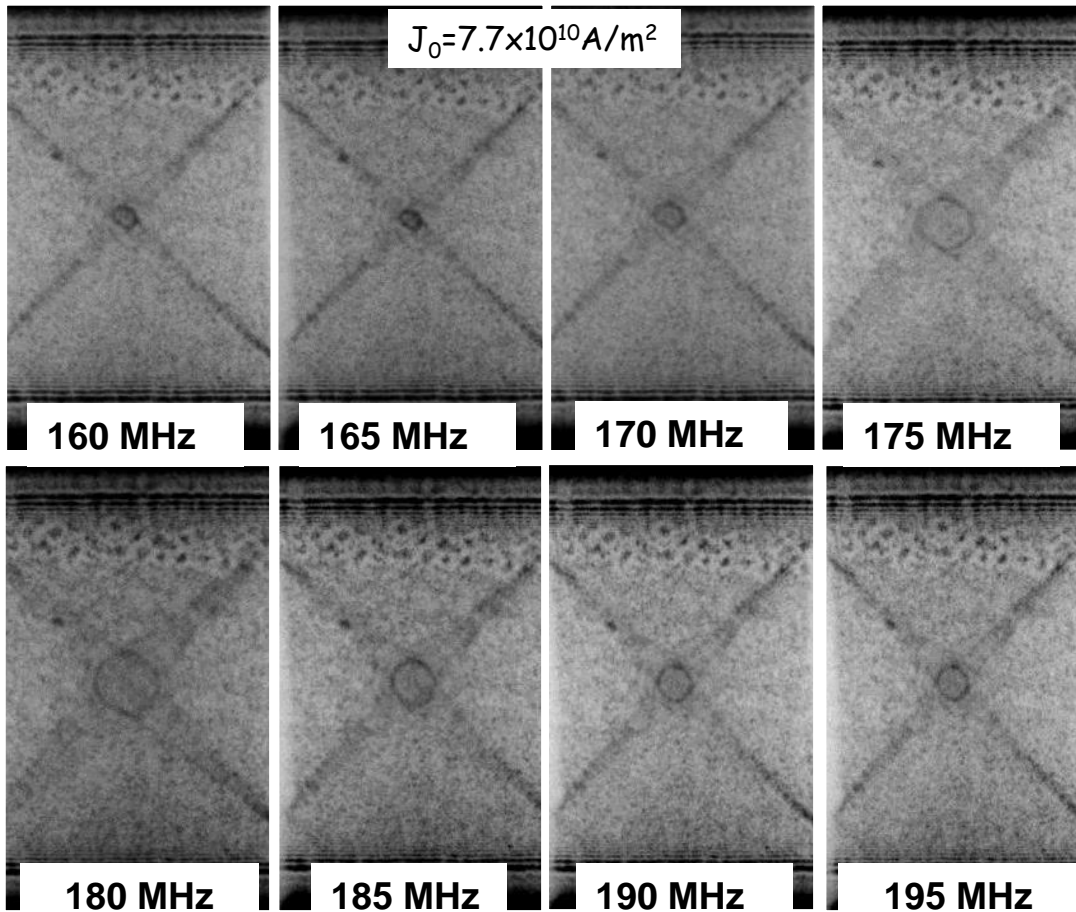


image

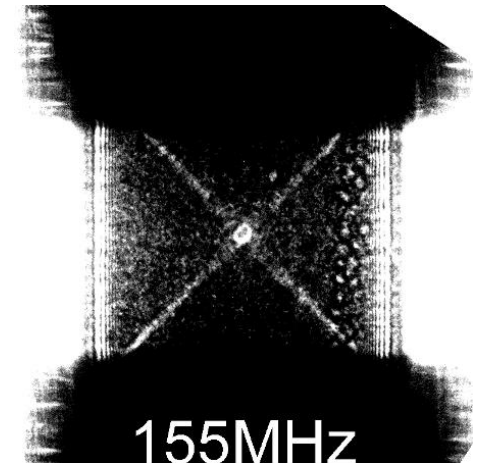
t B map

structure

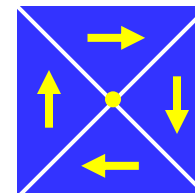
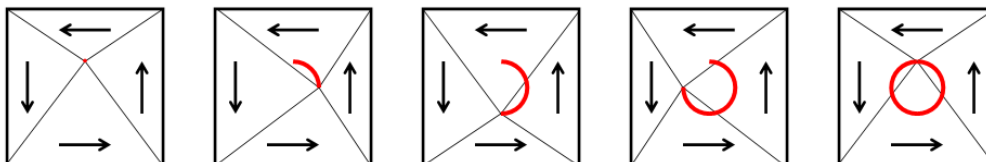
Imaging vortex-precession orbit via resonance excitation



Vortex dynamics in nanomagnet



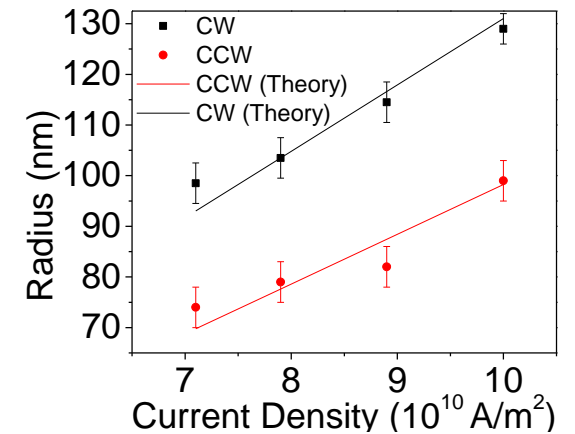
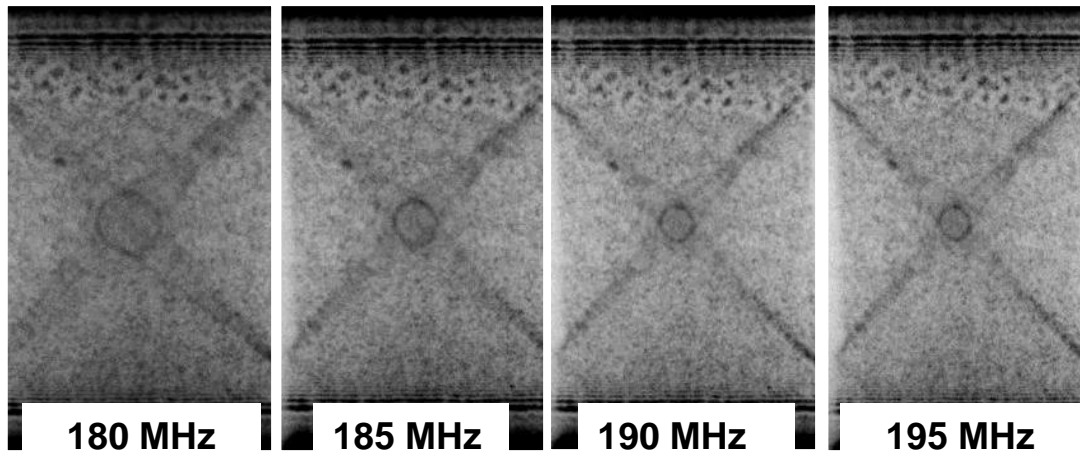
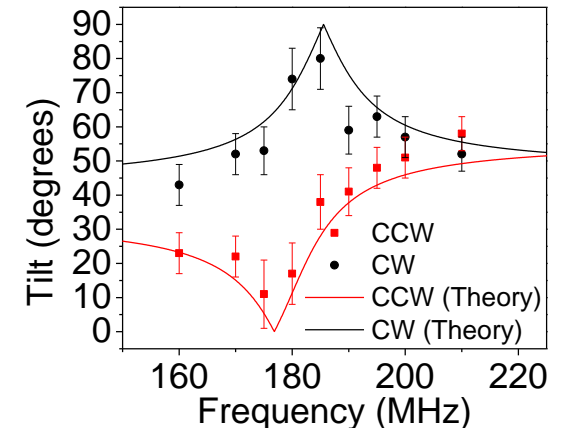
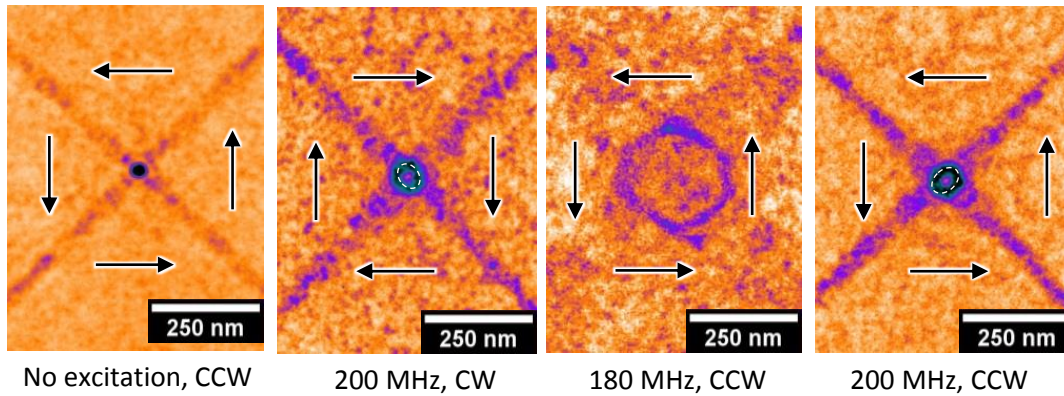
Direct observations of vortex precession orbit



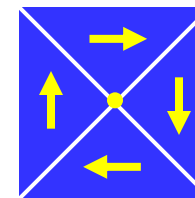
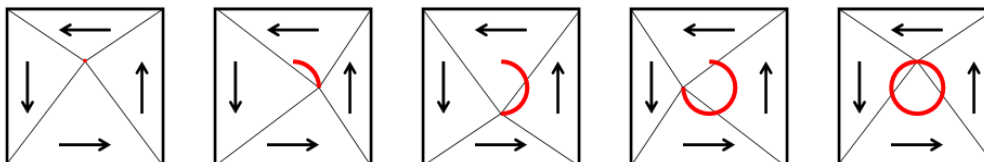
Zum Py square

Pollard et al Nature Comm.
3 1028 (2012)

Imaging vortex-precession orbit via resonance excitation



Direct observations of vortex precession orbit



Our goals: understanding strongly correlated materials

Challenges:

Coupling electronic-lattice system

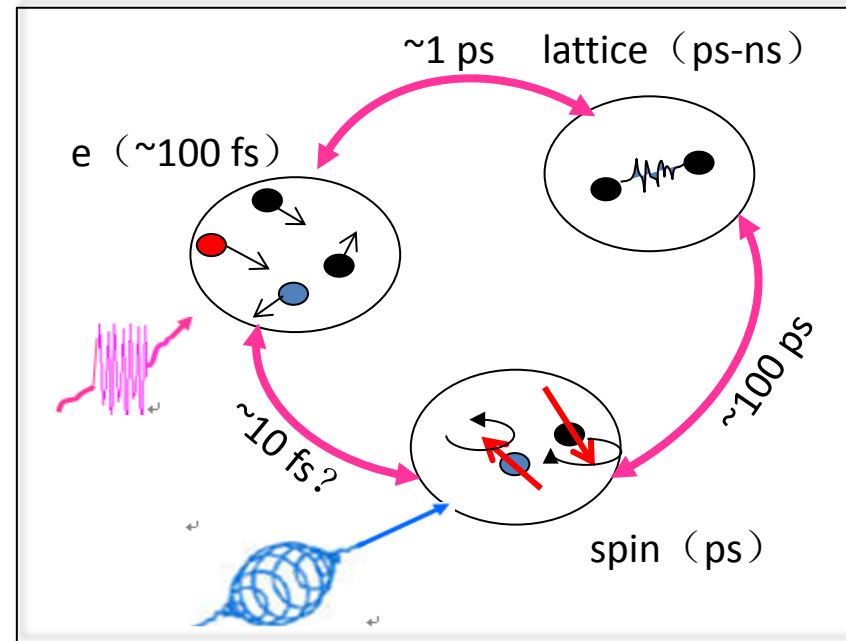
→ charge, orbital and spin order

Strong interplay between charge, spins, orbital and lattice

→ complex phase diagrams, exotic material properties

One solution:

Decouple the subsystems in the time domain and then observe the dynamics of subsystems separately.

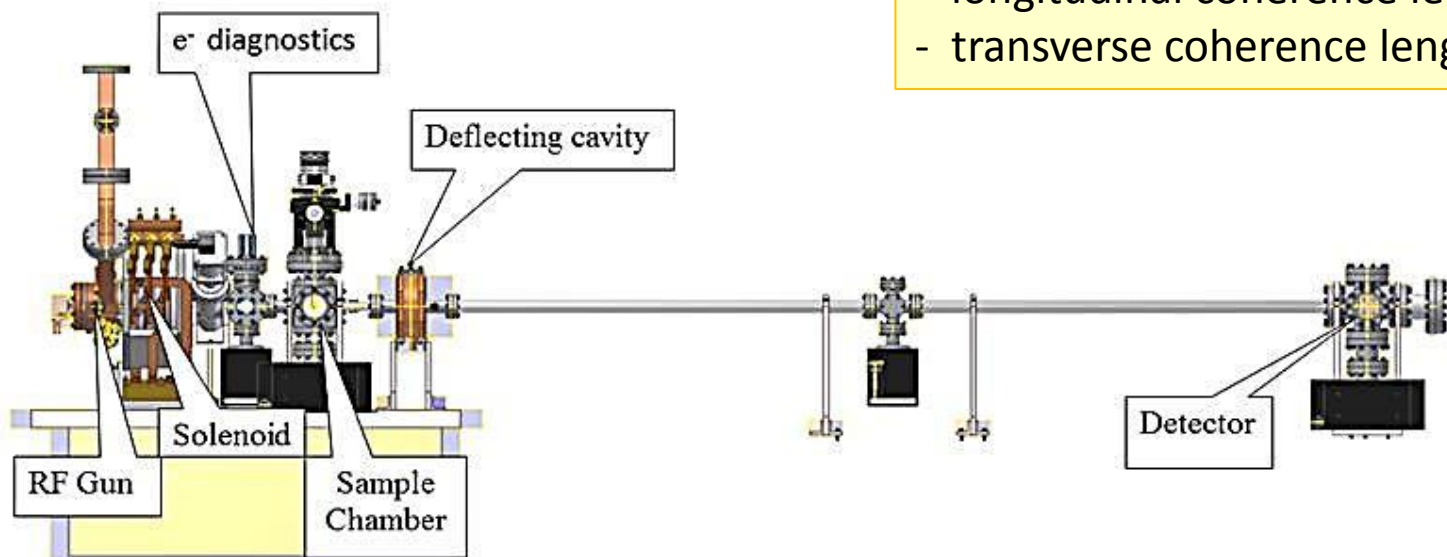


Ultrafast ED: better time resolution & simultaneously observe diverse degrees of freedom.

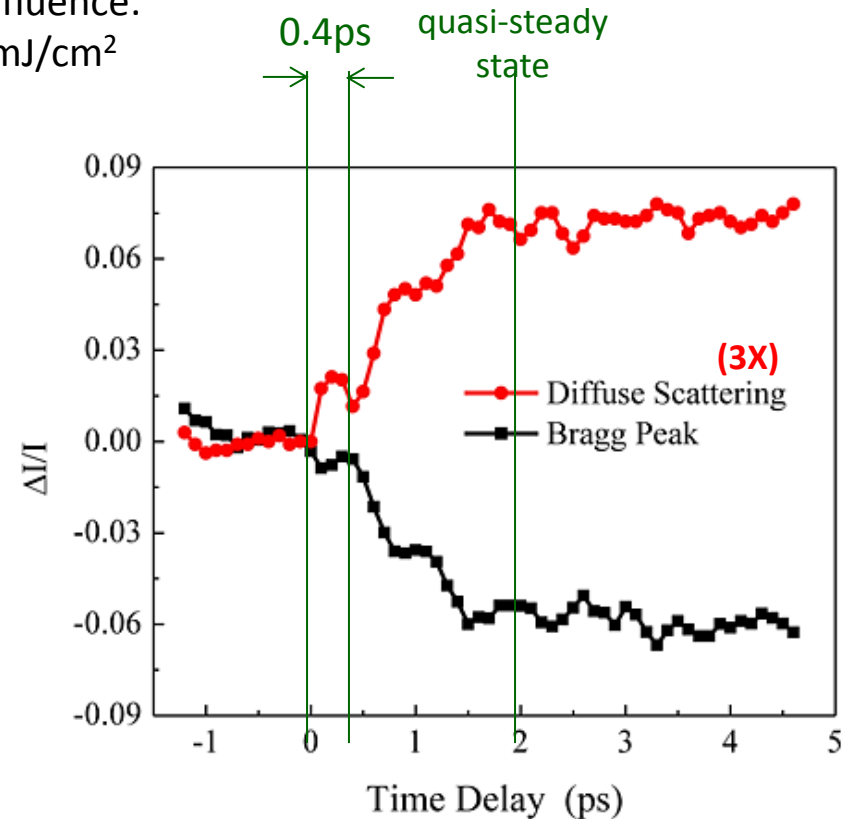
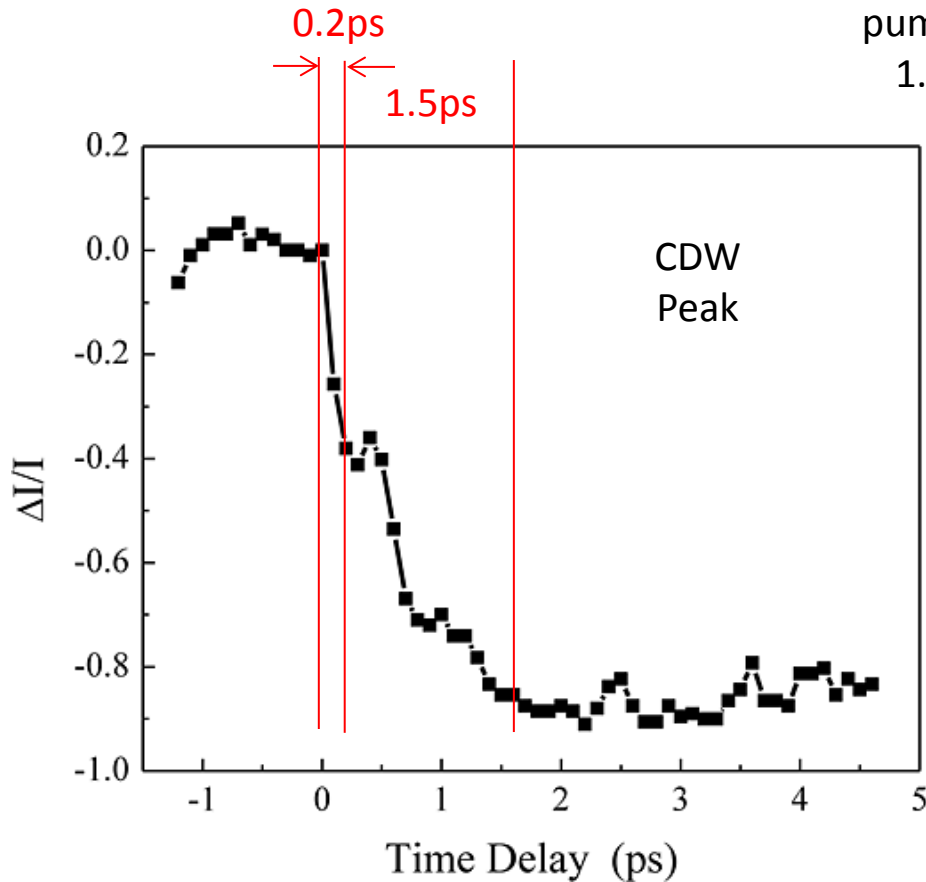
Ultrafast electron diffraction at BNL

Currently optimized at
2.8MeV with 120fs resolution

- 2-4 MeV electron energy
- 100 fs pulse, Hz repetition rate
- 10^6 electrons in a single pulse
- energy spread $<0.01\%$
- 30urad divergence
- beam size on detector 200um
- Synchronization of RF & laser <50 fs
- cryogenic capability
- longitudinal coherence length 1-2nm
- transverse coherence length ~ 10 nm



2H-TaSe₂

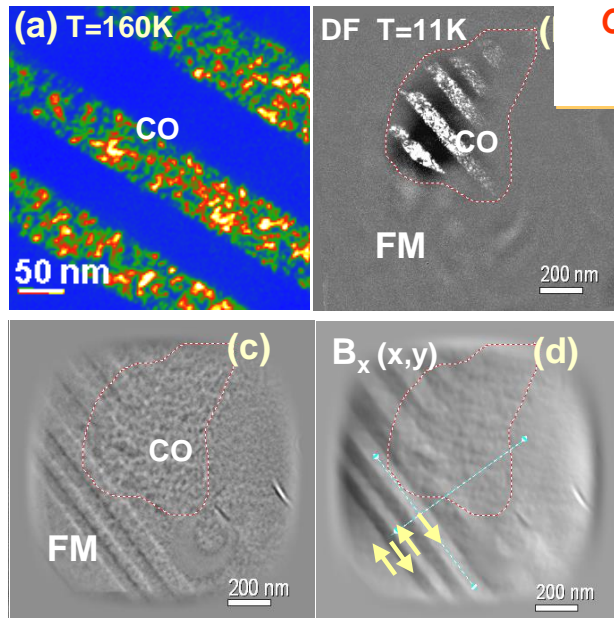
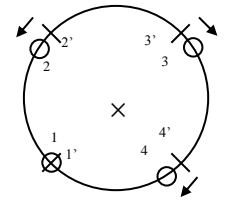
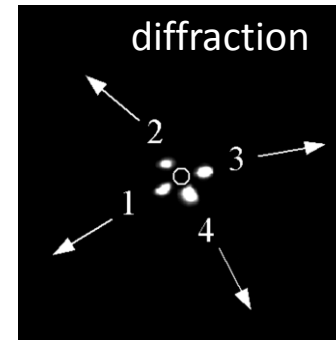
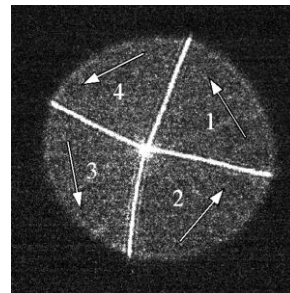
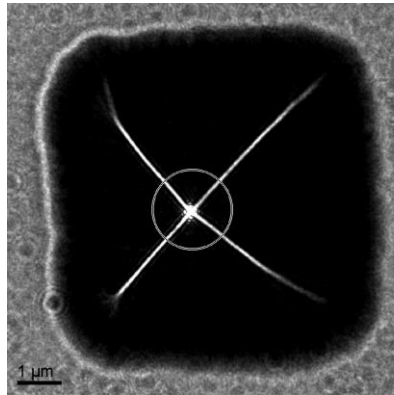


SP intensity reduced to ~ 0 , without obvious recovery in the following 50 ps

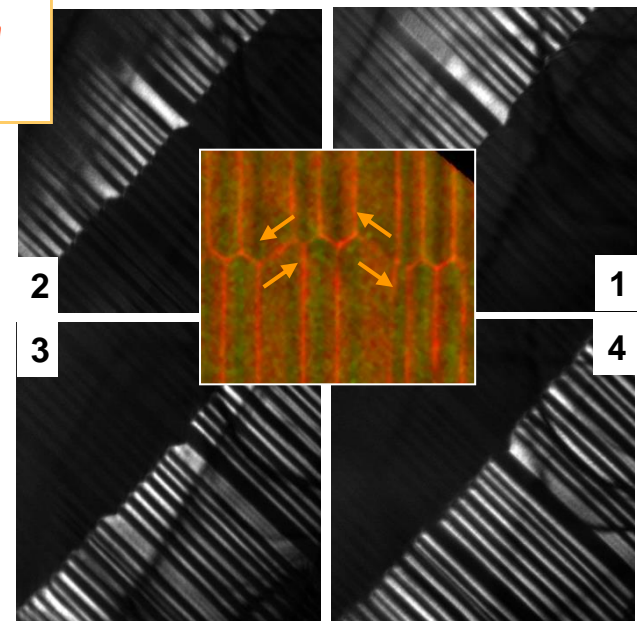
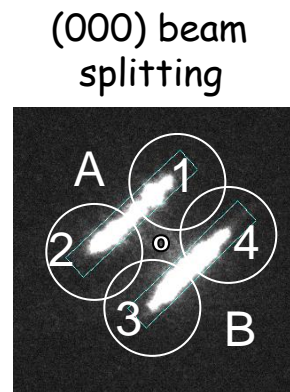
Coherent phonon: 2.5THz (~ 400 fs)

Ultrafast electron diffraction for spin dynamics ?

Split of transmitted and diffraction spots due to magnetic domains in permalloy



orbital-spin ordering
 $\text{La}_{1/4}\text{Pr}_{3/8}\text{Ca}_{3/8}\text{MnO}_3$



Acknowledgement

Atomic imaging: D. Su, H. Xin, H. Inada, J. Wall, L. Wu

Electron diffraction: L. Wu, C. Ma, J. Taftø

Holography: MG Han

Magnetic imaging: S. Pollard, V. Volkov, M. Malac

Ultrafast: XJ. Wang, P. Zhu, J. Hill, J. Cao

Supported by US DOE/BES

Thank you !

